Nuclear Physics B 380 (1992) 478–506
North-Holland

NUCLEAR
PHYSICS B

Neutrino astronomy and massive long-lived particles from the big bang

V.S. Berezinsky

Laboratori Nazionali del Gran Sasso (INFN), S.S. 17 bis Km. 18 + 910, 67010 Assergi (AQ), Italy
and
Physikalisches Institut der Universität Bonn, Nussallee 12, D-53 Bonn 1, Germany

Received 1 August 1991
(Revised 30 January 1992)
Accepted for publication 5 March 1992

We consider the neutrino flux from the decay of long-lived big-bang particles. The red-shift z_{tr} at which the neutrino transparency of the universe sets in is calculated as a function of neutrino energy: $z_{tr} \simeq 1 \times 10^5$ for TeV neutrinos and $z_{tr} \simeq 3 \times 10^6$ for 10 MeV neutrinos. One might expect the production of detectable neutrino flux at $z \lesssim z_{tr}$, but, as demonstrated in this paper, the various upper limits, most notably due to nucleosynthesis and diffuse X- and gamma-rays, preclude this possibility. Unless the particle decay is strongly dominated by the pure neutrino channel, observable neutrino flux can be produced only at the current epoch, corresponding to red-shift $z \approx 0$. For the thermal relics which annihilate through the gauge bosons of SU(3)× SU(2)×U(1) group, the neutrino flux can be marginally detectable at $0.1 < E_\nu < 10$ TeV. As an example of non-thermal relics we consider gravitinos. If gravitinos are the lightest supersymmetric particles (LSP) they can produce the detectable neutrino flux in the form of a neutrino line with energy $E_\nu = \frac{1}{2} M_G$, where M_G is the gravitino mass. The flux strongly depends on the mechanisms of R-parity violation. It is shown that heavy gravitinos ($M_G \lesssim 100$ GeV) can make up the dark matter in the universe.

1. Introduction

In this paper we shall discuss the diffuse neutrino radiation from the decays of cosmologically produced massive particles.

From the point of view of detection technique, neutrino astronomy covers the energy range from several MeV up to 10^7 GeV. The detection of low-energy (LE) neutrinos (10 MeV range) is connected mostly with the reaction $\bar{\nu}_e + p \to n + e^+$. The detection of ultra-high energy (UHE) neutrinos ($\sim 10^7$ GeV) is also connected with $\bar{\nu}_e$ neutrinos due to the reaction $\bar{\nu}_e + e^- \to W^- \to$ hadrons. However, we shall be mostly interested here in very high-energy (VHE) neutrinos of TeV energy range. These neutrinos can be effectively detected with the help of underground (underwater) muons produced in $\nu_\mu + N \to \mu +$ all scattering.

0550-3213/92/$05.00 © 1992 – Elsevier Science Publishers B.V. All rights reserved

VHE neutrino astronomy is based on [1] neutrino production by accelerated particles through production and subsequent decay of charged pions (kaons). An exceptional case is suggested in refs. [2,3] of high-energy neutrino production through the decay of massive long-lived particles from the big bang. This suggestion, very interesting and promising, was put forward in a very general form. In particular the physical properties of the decaying particles, including the relic concentration, were taken ad hoc. Here we shall present the quantitative discussion of the problem and obtain upper bounds on the neutrino fluxes and energies. In our consideration we take into account the neutrino absorption in the early universe (see also ref. [4]) and use the usual cosmological constraints on the massive long-lived particles, such as derived from nucleosynthesis, distortion of 2.7 K black-body radiation, isotropic X-ray radiation etc.

Our approach to the problem is the following. We shall consider the hypothetical X-particles taken as fermions with arbitrary mass m_X and lifetime τ_X, which decay as $X \to \nu +$ all ($X \to 3\nu$ will be considered as a possibility). For each energy $E_{\nu 0}$ of the neutrino at the present ($z = 0$) epoch, the moment t_a of absorption in the past due to $\nu\bar{\nu}$ scattering is calculated. It determines the range of τ_X ($\tau_X > t_a$) of interest. Then the relic concentration $n_X(t)$ is calculated, taking into account $X\bar{X}$ annihilation due to electroweak or strong interaction. The upper limits on neutrino energies and fluxes are imposed by big-bang nucleosynthesis, 2.7 K black-body radiation and/or diffuse X- and gamma-rays and the critical density of universe. Attention will be given mostly to VHE neutrinos ($E_{\nu 0} > 100$ GeV).

Our calculations are performed within the standard $\Omega = 1$ cosmology. Actually, very heavy particles with small enough annihilation cross section can dominate the density of the universe, until they decay. As the reader will see in the end of the paper, here such is not the case. It follows directly from the constraint $\rho_X(t_0) < \rho_{cr}(t_0)$. This inequality holds for $t_{eq} < t < t_0$ since both $\rho_{cr}(t)$ and $\rho_X(t)$ are proportional to $1/t^2$ (here t_{eq} and t_0 are the equilibrium time and the age of the universe). At $t < t_{eq}$ the inequality further strengthens since $\rho_{cr}(t) \propto t^{-2}$ as the energy density of relativistic particles, while $\rho_X(t) \propto t^{-3/2}$, as the energy density of non-relativistic particles.

The following cosmological values will be used throughout the paper: the critical density $\rho_c = 1.88 \times 10^{-29}\ h^2$ g/cm^3, where $h = H_0/(100\ \text{km} \cdot \text{Mpc}^{-1}\ \text{s}^{-1})$, the decoupling moment $t_{dec} = 3.6 \times 10^{12}\ h^{-1}$ s ($z_{dec} \approx 1.5 \times 10^3$); the equilibrium time $t_{eq} = 5.1 \times 10^{10}\ h^{-4}$ s ($z_{eq} \approx 2.5 \times 10^4\ h^2$), at which time the scaling factor $a(t)$ changes its time dependence from $a(t) \propto t^{1/2}$ to $a(t) \propto t^{2/3}$; the kinetic moment $t_{kin} \simeq 3 \times 10^5$ s ($z_{kin} \simeq 1 \times 10^7$), at which time the thermodynamic equlibrium for the photons breaks down, but kinetic equilibrium $e + \gamma \to e + \gamma$ is still supported; and, finally, the age of Universe $t_0 = 2.1 \times 10^{17}\ h^{-1}$ s.

Some parts of this work have been published in the form of a preprint [4] and a paper [5]. Some topics of this paper were also recently considered in refs. [6,7].

2. Neutrino absorption

Let us first consider the absorption of high energy neutrinos with the aim of finding the red-shift z_a up to which the universe is transparent for neutrinos with present ($z = 0$) energy $E_{\nu 0}$. The relevant processes are due to interaction with black-body neutrinos ν_{bb}: $\nu + \bar{\nu}_{bb} \to e^+ + e^-$, $\nu + \bar{\nu}_{bb} \to \mu^+ + \mu^-$, $\nu + \bar{\nu}_{bb} \to$ pions, etc.

Let us consider first $\nu_\mu + \bar{\nu}_\mu \to e^+ + e^-$ scattering. Its cross section is

$$\sigma(\epsilon_c) = \sigma_0(1 + p_c^2/3\epsilon_c^2)(p_c/m_e)(\epsilon_c/m_e), \tag{1}$$

where p_c and ϵ_c are the momentum and energy of electron in the c.m. system, m_e is the electron mass,

$$\sigma_0 = (2/\pi) f(\xi) G_F^2 m_e^2 = 1.11 \times 10^{-45} \text{ cm}^2, \tag{2}$$

G_F is the Fermi constant and $f(\xi)$ is a function of the Weinberg angle, $\xi = \sin^2\theta_W \approx 0.23$:

$$f_{\nu_\mu \bar{\nu}_\mu}(\xi) = 2\xi^2 - \xi + \tfrac{1}{4}.$$

With the cross section (1) and the known density of black-body neutrinos (antineutrinos) it is trivial to calculate the pathlength of high-energy neutrinos for arbitrary red-shift z as

$$l_\nu(\epsilon_\nu) = l_0 \epsilon_\nu^2 \phi^{-1}(\epsilon_\nu), \tag{3}$$

where $\epsilon_\nu = E_\nu/E_0$ is the dimensionless neutrino energy,

$$E_0 = m_e^2/kT = 1.57 \times 10^6 (1.93/T) \text{ GeV}, \tag{4}$$

$$l_0 = \frac{3\pi^2}{2\sigma_0}\left(\frac{c\hbar}{kT}\right)^3 = 2.45 \times 10^{42}\left(\frac{1.10^{-44} \text{ cm}^2}{\sigma_0}\right)\left(\frac{T}{1.93}\right)^{-3} \text{ cm}, \tag{5}$$

$$\phi(\epsilon_\nu) = \int_1^\alpha dx\, x^4\left(4 - \frac{1}{x^2}\right)(x^2 - 1)^{1/2} \ln(1 + e^{-x^2/\epsilon_\nu}), \tag{6}$$

T is the temperature of the neutrino gas, which is $T_0 = 1.93$ K at $z = 0$ and $T = (1 + z)T_0$ at red-shift z. The asymptotic expressions for $\phi(\epsilon_\nu)$ are given by

$$\phi(\epsilon_\nu) = 4\epsilon_\nu^3, \qquad \epsilon_\nu \gg 1, \tag{7a}$$

$$\phi(\epsilon_\nu) = \frac{3\sqrt{\pi}}{4}\epsilon_\nu^{3/2} e^{-1/\epsilon_\nu}\left(1 + \tfrac{11}{4}\epsilon_\nu + \tfrac{65}{32}\epsilon_\nu^2 + \ldots\right), \qquad \epsilon_\nu \ll 1. \tag{7b}$$

The values of $\phi(\epsilon_\nu)$ for intermediate values of ϵ_ν are given in table 1.

TABLE 1
The values of $\phi(\epsilon_\nu)$

ϵ_ν	0.3	0.5	1	3	10
$\phi(\epsilon_\nu)$	1.54×10^{-2}	0.174	2.46	90.0	3.65×10^{3}

For the reaction $\nu+\bar{\nu}\to f+\bar{f}$ where $f=$ e, μ, τ, u, d, s, c etc. one should substitute m_f instead of m_e in eqs. (1)–(7) and calculate $f(\xi)$ for the particular process (in fact, for the quarks a more sophisticated consideration is needed). The interesting observation is that the asymptotic ($\epsilon_\nu \gg 1$) formula for the pathlength,

$$l_\nu(\epsilon_\nu) = (3\pi^2/8\sigma_0)(E_0/E_\nu)(c\hbar/kT)^3, \tag{8}$$

does not depend on m_f since both σ_0 and E_0 are proportional to m_f^2. Therefore, the total pathlength of neutrinos due to production of all f-particles with masses satisfying $\epsilon_\nu \gg m_f^2/m_e^2$ is

$$l_\nu^{\mathrm{tot}}(\epsilon_\nu) = \left(3\pi^2/8\sum\sigma_{0f}\right)(c\hbar/kT)^3(E_0/E_\nu), \tag{9}$$

where E_0 and σ_{0f} are defined through the electron mass m_e according to eqs. (1), (2), (4), and the function $f(\xi)$, which we calculated for the different $\nu+\bar{\nu}\to f+\bar{f}$ channels are listed in table 2. The third row in table 2 ($\nu+\bar{\nu}\to$ pions) corresponds to the sum of the cross sections $\nu+\bar{\nu}\to \mathrm{u}+\bar{\mathrm{u}}$ and $\nu+\bar{\nu}\to \mathrm{d}+\bar{\mathrm{d}}$, where $\cos\theta_c = 1$ was used.

Therefore, in the limit $\epsilon_\nu \gg m_\pi^2/m_f^2$ relevant for further calculations, the absorption lifetime of neutrinos in the epoch with red-shift z is

$$\tau_\nu(E_{\nu 0}, z) = \tau_0(1+z)^{-5}E_0/E_{\nu 0}, \tag{10}$$

where $E_{\nu 0}$ is the neutrino energy at $z=0$, $E_0 = m_e^2/kT_0 = 1.57\times10^6$ GeV and

$$\tau_0 = \frac{3\pi^2}{8c\sum\sigma_{0f}}\left(\frac{\hbar c}{kT_0}\right)^3 = 2.05\times10^{31}\frac{1\times10^{-44}\ \mathrm{cm}^2}{\sum\sigma_{0f}}\mathrm{s}. \tag{11}$$

TABLE 2
The function $f(\xi)$ from eq. (2) for different processes

	e^+e^-	$\mu^+\mu^-$	pions
$\nu_\mu\nu_\mu$	$2\xi^2-\xi+\frac{1}{4}$	$2\xi^2+\xi+\frac{1}{4}$	$\frac{10}{9}\xi^2-\xi+\frac{1}{2}$
$\nu_e\bar{\nu}_e$	$2\xi^2+\xi+\frac{1}{4}$	$2\xi^2-\xi+\frac{1}{4}$	$\frac{10}{9}\xi^2-\xi+\frac{1}{2}$

The red-shift z_a at which the absorption sets in for the neutrino with present ($z=0$) energy $E_{\nu 0}$ can be found from the condition $\tau_\nu(E_{\nu 0}, z) \sim H^{-1}(z)$, where $H(z)$ is the Hubble constant in the relevant cosmological epoch. Taking into account that the epoch of neutrino absorption, t_a, occurs earlier than the equilibrium time t_{eq} one easily finds:

$$z_a \simeq (t_{eq}/t_0)^{1/9}\left(\tfrac{3}{4}H_0\tau_0 E_0/E_{\nu 0}\right)^{1/3}$$

$$= 7.9\times 10^4\left(\frac{10^{-44}\ \mathrm{cm}^2}{\sum\sigma_{0f}}\right)^{1/3}\left(\frac{E_{\nu 0}}{1\ \mathrm{TeV}}\right)^{-1/3}, \tag{12}$$

$$t_a \simeq 5.4\times 10^9\left(\sum\sigma_{0f}/10^{-44}\ \mathrm{cm}^2\right)^{2/3}(E_{\nu 0}/1\ \mathrm{TeV})^{2/3}\ \mathrm{s}. \tag{13}$$

It is easy to verify that eq. (12) does not contain h.

To calculate $\sum\sigma_{0f}$ for eqs. (12) and (13) we must evaluate ϵ_ν and the c.m. energy squared, s, at the epoch of absorption. They are:

$$\epsilon_\nu(z_a) \simeq 1.0(m_f/1\ \mathrm{GeV})^{-2}(E_{\nu 0}/1\ \mathrm{TeV})^{1/3}\left(\sum\sigma_{0f}/10^{-44}\ \mathrm{cm}^2\right)^{-2/3}, \tag{14}$$

$$s(z_a) \simeq 5.6(E_{\nu 0}/1\ \mathrm{TeV})^{1/3}\left(\sum\sigma_{0f}/10^{-44}\ \mathrm{cm}^2\right)^{-2/3}\ \mathrm{GeV}^2. \tag{15}$$

Therefore, for muon neutrinos with $E_{\nu 0}\simeq 1$ TeV the contribution comes from $\nu_\mu+\bar\nu_\mu\to e^+ + e^-$, $\nu_\mu+\bar\nu_\mu\to\mu^+ +\mu^-$ and $\nu_\mu+\bar\nu_\mu\to$ pions. Then from table 2 one finds $\sum f_f(\xi)=(46/9)\xi^2-\xi+1\simeq 1$ and $\sum\sigma_{0f}=(2/\pi)\ G_F^2 m_e^2 = 8.8\times 10^{-45}\ \mathrm{cm}^2$. For electron antineutrinos with $E_\nu\simeq 10$ MeV, only $\nu_e+\bar\nu_e\to e^+ + e^-$ contributes to the opacity and $\sum\sigma_{0f}=5.2\times 10^{-45}\ \mathrm{cm}^2$.

Up to now we neglected the neutrino mass. Can it influence the absorption? The neutrino mass m_ν is essential for absorption only if

$$z_a 3.15kT_0 \lesssim m_\nu, \tag{16}$$

or

$$m_\nu \gtrsim 52.4(T_0/1.9\ \mathrm{K})\ \mathrm{eV}. \tag{17}$$

In the frame of the see-saw mechanism, only τ-neutrinos can satisfy this condition. It is trivial to estimate τ-neutrino absorption due to $\nu_\tau+\bar\nu_\tau\to f+\bar f$, assuming the maximum τ-neutrino mass $m_\nu=100$ eV. The red-shift for the absorption epoch for the present day energy $E_{\nu 0}$ is

$$z_a = \left(\tfrac{3}{4}H_0\tau_0\tilde E_0/E_{\nu 0}\right)^{1/2}(t_{eq}/t_0)^{1/6},$$

where

$$\tilde{E}_0 = m_e^2/m_\nu = 2.6(100\ \text{eV}/m_\nu)\ \text{GeV},$$

$$\tau_0 = 2/(\sigma_0 c n_{\nu 0}), \qquad n_{\nu 0} = 54.5\ \text{cm}^{-3}.$$

For $\tau_0 = 1 \times 10^{-44}\ \text{cm}^2$ we obtain

$$z_a = 7.0 \times 10^4 (E_{\nu 0}/1\ \text{TeV})^{-1/2} (m_\nu/100\ \text{eV})^{-1/2}. \tag{18}$$

Comparison with eq. (12) shows that this effect is not significant even for the largest possible neutrino mass.

3. Elastic neutrino–neutrino scattering

Elastic $\nu\nu$ scattering off black-body neutrinos results in energy loss of the incident neutrino. Let us consider a neutrino with energy $E_{\nu 0}$ at observation ($z = 0$). For the epochs when the scattering effectively sets in, the neutrino energy at production increases exponentially with red-shift. The red-shift z_{el} when the exponential grow sets in, can be found by equating the relative energy loss of the neutrino with the Hubble constant at that epoch:

$$\frac{1}{E}\frac{dE}{dt} = H(t). \tag{19}$$

Let us now proceed to the cross sections and the fraction of energy loss for higher energy ν_i neutrinos (the indices i and k run through e, μ and τ). The scattering channels fall into the three categories: (i) $\nu_i + \nu_k \to \nu_i + \nu_k$; (ii) $\nu_i + \bar{\nu}_k \to \nu_i + \bar{\nu}_k$ with $i \neq k$; (iii) $\nu_i + \bar{\nu}_i \to \nu_k + \bar{\nu}_k$. The last process goes through s- and t-channels. The cross sections for these three processes are:

$$\sigma_{(i)} = \frac{2}{\pi} G_F^2 \epsilon_c^2, \qquad \sigma_{(ii)} = \frac{2}{3\pi} G_F^2 \epsilon_c^2, \qquad \sigma_{(iii)} = \frac{4}{\pi} G_F^2 \epsilon_c^2, \tag{20}$$

where ϵ_c is the neutrino energy in the c.m. system. Further on we shall use the product of the cross section and the number of flavours, f, of the target neutrinos participating in the scattering ($f_{(i)} = 3$, $f_{(ii)} = 2$ and $f_{(iii)} = 1$). Accordingly, for the space density of the target neutrinos we shall use the single-flavour value.

The c.m. angular distribution of neutrinos in the process (i) is isotropic. The fraction of energy lost in the laboratory system is $\langle \Delta E/E \rangle = \frac{1}{2}$. For the other two

processes the angular distribution is proportional to $(1-\cos\theta_c)^2$ and the fraction of energy lost is $\frac{3}{4}$. In this case most of the energy is carried away by the target neutrino. If the change of neutrino flavour is not taken into account, the fraction of energy lost is $\frac{1}{4}$. The value averaged over all three processes is 13/34.

The product of the cross section (with the target flavour taken into account) and the mean fraction of energy lost can be written as

$$(\Delta E/E)\sigma(\epsilon_c) = \sigma_0(\epsilon_c/m_e)^2, \tag{21}$$

where

$$\sigma_0 = \frac{13}{3\pi} G_F^2 m_e^2 = 1.9\times 10^{-44}\ \text{cm}^2 \tag{22}$$

(to be compared with $\sum\sigma_{0f} \simeq 1\times 10^{-44}$ cm^2 used in eqs. (11)–(15)).

The energy-loss length $l_{el}(\epsilon_\nu)$, defined as

$$l_{el}^{-1} \equiv \left\langle \frac{1}{E_\nu}\frac{dE_\nu}{dl}\right\rangle = \int d\Omega \int d\epsilon'\, n_\nu(\epsilon')\left\langle\frac{\Delta E}{E}\right\rangle \sigma(\epsilon_c)(1-\cos\theta),$$

is given by:

$$l_{el}(\epsilon_\nu) = \chi l_0/\epsilon_\nu, \tag{23}$$

where

$$l_0 = \frac{\pi^2}{2\sigma_0}\left(\frac{c\hbar}{kT_0}\right)^3 = 4.31\times 10^{41}(T_0/1.93\ \text{K})\ \text{cm},$$
$$1/\chi = \tfrac{1}{2}\int_0^\alpha dx\, x^2 \ln(1+e^{-x}) = 0.945, \tag{24}$$

and $\epsilon_\nu = E_\nu/E_0$ as in eq. (3).

Using $E_\nu(z) = (1+z)E_{\nu 0}$ and $l_{el}(z) = 1.06 l_0(E_0/E_{\nu 0})(1+z)^{-5}$, one obtains from eq. (19):

$$z_{el} \approx \left(\frac{t_{eq}}{t_0}\right)^{1/9}\left(8\frac{l_0}{c}H_0\frac{E_0}{E_{\nu 0}}\right)^{1/3} = 7.1\times 10^4(E_{\nu 0}/1\ \text{TeV})^{-1/3}, \tag{25}$$

which practically coincides with z_a (see eq. (12)). The largest difference is found for 10 MeV electron neutrinos: $z_a = 4.6\times 10^6$ and $z_{el} = 3.3\times 10^6$.

The influence of neutrino mass on elastic scattering is less than the effect on absorption, since in the former case there is no summation over neutrino flavours. For the most important case $\nu_i + \nu_\tau \to \nu_i + \nu_\tau$ it is easy to obtain:

$$z_{el} = \left(\tfrac{3}{4} H_0 \tau_0 \tilde{E}_0 / E_{\nu 0}\right)^{1/2} \left(t_{eq}/t_0\right)^{1/6} = 1.1 \times 10^5 (m_\nu / 100 \text{ eV})^{-1/2}, \quad (26)$$

where

$$\tau_0 = \frac{2}{\sigma_0 c n_{\nu 0}} \frac{\tilde{E}_0}{E_\nu},$$

$$\sigma_0 = G_F^2 m_e^2 / \pi = 4.4 \times 10^{-45} \text{ cm}^2.$$

Therefore, it follows from the two sections above that the horizon for VHE ($E_{\nu 0} \simeq 1$ TeV) and low-energy ($E_{\nu 0} \simeq 1$ MeV) neutrino detectors is limited to red shifts $z \simeq 10^5$ and $z < 3 \times 10^6$, respectively.

4. Particles

From the above consideration it follows that the lifetime of the X-particles, the neutrino parent, must exceed 10^{10} s for VHE neutrino astronomy. On the other hand, these particles must be massive. In particular, a particle with lifetime $\tau_X \simeq t_a \simeq 10^{10}$ s should have a mass $m_X \simeq E_{\nu 0} z_a \simeq 10^8$ GeV. The larger τ_X, the lower can be m_X. The realistic case, as will be shown from the calculations, corresponds to $\tau_X > t_0$ and $m_X \simeq 100$–1000 GeV.

Can such massive long-lived particles exist in the modern theory? We shall give here two examples.

The first one consists of assigning the X-particle to the fourth generation of GUT. To provide the large lifetime τ_X, no mixing with the light particles should be allowed in fourth generation. An interesting possibility consists in identifying X with the D-quark, an analogue of d- and s-quarks. If the D-quark is the second lightest (after neutrino ν_4) fermion in the fourth generation, it decays through interaction of five-plets of right-handed components mediated by exchange of superheavy $Y^{1/3}$ gauge bosons: $X \to \nu_4 + q + \nu$, where q is a d-, s- or b-quark. The branching ratio of neutrino decay is $b_\nu \simeq \frac{1}{3}$. The fraction of energy transferred to electrons and photons, (an important quantity for further discussion) is more difficult to estimate. At the moment of decay, D-quarks exist in the form of colourless hadrons $\bar{d}D$, $\bar{u}D$, udD etc, whichever is the lightest one. The decay $D \to \nu_4 + q + \nu$ results in the formation of an unstable hadronic state with excitation energy $E \simeq \frac{1}{3} m_D$. About half of this energy is transferred in the processes of de-excitation and decays to electrons and photons and, therefore, the fraction of

energy transferred to them is $f_{em} \simeq \frac{1}{6}$. If the three-fermion decay of the X-particle is mediated by a gauge boson $Y^{1/3}$ with GUT unification mass $m_Y \simeq 10^{16}$ GeV, its lifetime is:

$$\tau_X \simeq 10^{11}(m_X/10^7 \text{ GeV})^{-5}(m_Y/10^{16} \text{ GeV})^4 \text{ s}. \tag{27}$$

Therefore, the particles lighter than 10^7 GeV can have lifetimes long enough to be the parents of VHE/UHE neutrinos.

More realistically, such a particle can be the lightest particle of some hidden sector with discrete symmetry. Breaking of this symmetry provides the decay of the lightest particle. Ellis et al. [8] have recently considered the hidden sector particles – cryptons – which can be quasistable and thus produce VHE neutrinos. A less speculative example is given by supersymmetry with very weak R-parity violation. The lightest supersymmetric particle can have a lifetime longer than the age of the universe and produce an observable VHE neutrino flux.

Another example is given by a particle which decays due to gravitational interaction. A natural case, the gravitino, will be considered here explicitly.

We shall subdivide the neutrino parents into the two groups: the equilibrium and the non-equilibrium relics. The former, to which we shall refer as X-particles, were in thermal equilibrium in the early universe. The cross section for the latter group is so small that equilibrium was not reached at any age of the universe.

The present abundance of thermalized relics depends on the cross section of $X\overline{X}$ annihilation. In the general case of large m_X it can be written as

$$\sigma v = A\alpha^2/m_X^2, \tag{28}$$

with $\alpha = 1 \times 10^{-2}$ and A is to be calculated taking into account the specific properties of the X-particles. We shall impose here the restriction, that $X\overline{X}$ annihilation is mediated by a gauge boson of the $SU(3) \times SU(2) \times U(1)$ group.

In the aforementioned case $X = D$, the annihilation proceeds through gluon exchange. The cross section of the $X_i\overline{X}_j$ annihilation ($i = 1, 2, 3$ is the colour index) into a pair of the light quarks is $\sigma(X_i\overline{X}_j) \simeq \alpha_s^2(4m_X^2)/m_X^2$, where $\alpha_s(Q^2)$ is the QCD coupling constant. In SUSY $SU(5)_{min}$, $\alpha_s(Q^2) \simeq 0.084$ at $m_X \simeq 10^3$ GeV. Summing over six quarks we obtain $A \simeq 70$ at $m_X \simeq 10^3$ GeV.

In the case when X is a fourth generation electron or neutrino, $X\overline{X}$ annihilation is mediated by photons and Z^0 bosons or by the Z^0 bosons alone, respectively. The straightforward calculations for the process $X\overline{X} \to f\bar{f}$, where f is a light fermion, result in the following expression for A:

$$A = \frac{\pi}{16} 10^4 \alpha_{em}^2(4m_X^2) \sum_f \sum_{J,I=L,R} \left(e_X e_f + \frac{Q_{fI}Q_{fJ}}{\sin^2\theta_W \cos^2\theta_W} \right)^2, \tag{29}$$

where e_X and e_f are the electric charges of X and f; $Q = T_3 - e \sin^2\theta_W$, and θ_W is the Weinberg angle. In eq. (22) we assume that f-fermions are relativistic, $m_X > m_Z$ and the sum runs over left (L) and right (R) states and over all fermions in three generations.

In the case of the SUSY $SU(5)_{min}$ model with $\alpha_{em}(4m_X^2) = 9.2 \times 10^{-3}$ for $m_X = 1 \times 10^3$ GeV, one obtains from eq. (22) $A = 4.7$ for the fourth generation electron and $A = 2.8$ for the fourth generation neutrino. We gave here these results just for completeness, our task, in fact, does not require such an accuracy.

Let us turn now to the non-thermalized relics and consider gravitinos as the most realistic example. To solve the hierarchy problem the gravitino must have a mass $m_G \simeq 100$ GeV. We shall take this value for the normalization, keeping in mind that larger masses are also possible. Unless it is the lightest supersymmetric particle (LSP), the gravitino lifetime, $\tau_G \simeq m_{Pl}^2/m_G^3 \simeq 3(100\ \text{GeV}/m_G)^3$yr is too short for the production of high-energy neutrinos ($m_{Pl} = 1.2 \times 10^{19}$ GeV is the Planck mass). In the case where the gravitino is the LSP its lifetime depends on the mechanism of R-parity violation and generally speaking it can be made arbitrarily long. In particular, in ref. [9] the gravitino lifetime is taken as 2×10^6 yr for $m_G \simeq 100$ GeV. For a review of mechanisms of R-parity breaking, see ref. [10].

At the end of the inflation stage, the gravitino density is diluted to a negligibly small value. However, the gravitinos are regenerated again during the reheating phase which follows the inflation stage. The cross section of gravitino production in the reactions $g + g \to \tilde{g} + G$, $g + \tilde{g} \to g + G$, $\gamma + e \to \tilde{e} + G$ etc., is $\sigma_{pr} \sim \alpha(m_G)/m_{Pl}^2$ [9,11,12] where α is the coupling constant. The cross section of gravitino annihilation is very small, $\sigma_{ann} \simeq N_f m_G^2/m_{Pl}^4$, where N_f is the number of final states, and therefore the relative gravitino concentration $Y = n_G/n_\gamma$ increases with time as $dY/dt \simeq \sigma_{pr} N(T) n_\gamma$, where $N(T)$ is the number of unfrozen degrees of freedom. At $t \simeq H^{-1}(T)$, where H is the Hubble constant, Y reaches the value $Y_R \simeq \sigma_{pr} N_R n_\gamma(T_R) H^{-1}(T_R)$ and then changes but a little, due to the decrease of $N(T)$ with time. The reheating values are marked by index R. More explicitly, using $n_G(t)/n_\gamma(t) = Y_R N(T)/N_R$ we obtain

$$n_G(t)/n_\gamma(t) = 0.24\left(\frac{45}{16\pi^3}\right)^{1/2} \frac{\alpha(T_R)}{m_{Pl}} \frac{N(T)}{N_R^{1/2}} T_R$$

$$= 7 \times 10^{-2} \alpha(T_R) \frac{N(T)}{N_R^{1/2}} \frac{T_R}{m_{Pl}}. \tag{30}$$

Therefore the space density of gravitinos is given in terms of the reheating temperature. Below we shall derive the upper bounds on the reheating temperature, but a remark is in order now. Unlike in the discussion in the past [11] we do not need a reheating temperature as high as $T_R \simeq 10^{13}$–10^{15} GeV since baryosynthesis can take place at a low temperature much later [13].

5. The neutrino flux

We turn now to the calculations of the remnant concentration n_X of X-particles and of the neutrino flux produced by their decays. The standard calculations [14] for n_X with the annihilation cross section given by eq. (28) results in

$$n_X(t) = \left(x_f^2 m_X^3/K\right)(t_f/t)^{3/2} \exp(-t/\tau_X), \qquad t < t_{eq}, \tag{31}$$

$$n_X(t) = \left(x_f^2 m_X^3/K\right)(t_f/t_{eq})^{3/2}(t_{eq}/t)^2 \exp(-t/\tau_X), \qquad t > t_{eq}. \tag{32}$$

Here, $T_f = x_f m_X$ is the freezing temperature, t_f is the freezing time:

$$t_f = 1.7 \times 10^{-11}(0.1/x_f)^2 m_3^{-2} N_{200}^{-1/2} \text{ s}, \tag{33}$$

N_f is the number of degrees of freedom at the freezing temperature, $N_{200} = N_f/200$ and

$$K = \frac{\alpha^2}{0.8} A \left(\frac{45}{4\pi^3}\right)^{1/2} \frac{\sqrt{N_f}}{N(t)} \frac{m_{Pl}}{m_X}. \tag{34}$$

We have modified the standard calculations [14], introduce, according to the recipe given in ref. [11], the factor $N(t)/N_f$ which describes the reheating of photon gas due to the annihilation of the freezing components and the correction factor 0.8 given by numerical calculations. Since further on we will be interested only in the epochs after neutrino transparency sets in ($t > 3 \times 10^9$ s), we can put in eq. (34) $N(t) = 43/11$ (it is composed of $\frac{43}{4}$, $\frac{11}{2}$ and 2), which gives

$$K \approx \frac{\alpha^2}{3.2} A \left(\frac{45}{4\pi^3}\right)^{1/2} N_f^{1/2} \frac{m_{Pl}}{m_X} = 6.5 \times 10^{12} \tfrac{1}{2} A m_3^{-1} N_{200}^{1/2}, \tag{35}$$

The values of x_f as a function of m_3 are given in table 3. The neutrino flux at the present epoch can be calculated as

$$I_\nu(t_0) = \frac{c}{4\pi} b_\nu \int_{t_a}^{t_0} \frac{dt}{\tau_X} n_X(t) \frac{a^3(t)}{a^3(t_0)}, \tag{36}$$

TABLE 3
The values of x_f as a function of m_3

m_3	0.63	6.0	2×10^2	2×10^3	1×10^4	2×10^5
x_f	0.045	0.050	0.060	0.070	0.080	0.10

where b_ν is the neutrino branching ratio. For the most interesting case, $t_a \ll \tau_X \ll t_0$, $I_\nu(t_0) = (c/4\pi) b_\nu n_X(t_0)$ since all X-particles decay, each leaving behind b_ν neutrinos. The neutrino flux can conveniently be given in terms of the standard flux

$$I_0 \equiv \frac{c}{4\pi} b_\nu x_f^2 \frac{m_X^3}{K} \left(\frac{t_f}{t_0}\right)^{3/2} \left(\frac{t_{eq}}{t_0}\right)^{1/2} \approx 9 \times 10^{-2} b_\nu m_3 \frac{0.1}{x_f} N_{200}^{-5/4} \text{ cm}^{-2} \text{ s}^{-1} \text{ sr}^{-1}, \tag{37}$$

$$I_\nu(t_0) = I_0 \exp(-t_a/\tau_X), \qquad \text{at } \tau_X \ll t_a, \tag{38a}$$

$$I_\nu(t_0) = I_0, \qquad \text{at } t_a \ll \tau_X \ll t_0, \tag{38b}$$

$$I_\nu(t_0) = I_0 t_0/\tau_X, \qquad \text{at } \tau_X \gg t_0. \tag{38c}$$

To evaluate the differential neutrino flux $I_\nu(E)$, one can divide the total neutrino flux by the neutrino energy

$$E_\nu \simeq m_3 \times 10^3/(1+z)_{\tau_X} \text{ GeV}, \tag{39}$$

where $(1+z)_{\tau_X}$ is the red-shift which corresponds to the time $t = \tau_X$. Then for $t_a \ll \tau_X \ll t_0$ we obtain

$$I_\nu(E) = 2.6 \times 10^{-4} (1+z)_{\tau_X} b_\nu \frac{0.1}{x_f} N_{200}^{-5/4} \text{ cm}^{-2} \text{ s}^{-1} \text{ sr}^{-1} \text{ GeV}^{-1}. \tag{40}$$

For $\tau_X \gg t_0$ the flux is t_0/τ_X times smaller.

The neutrino flux (40) does not depend on m_X. It follows from $n_\nu(t_0) = b_\nu n_X(t_0)$ (see the explanation after eq. (36)) and the well-known ratio $n_X(t_0)/n_\gamma(t_0) \sim m_X$. Since E_ν is also proportional to m_X, the differential flux does not depend on it.

The various physical phenomena which are considered below do not restrict the neutrino flux directly if the particle lifetime τ_X is fixed. They put an upper limit on the neutrino energy E_ν. The flux (40) retains the same value but is shifted to lower energies.

6. The upper limits on neutrino energies and fluxes

We shall consider here the most restrictive upper limits which follow from (i) the critical density; (ii) the distortion of the 2.7 K microwave radiation; (iii) the photoproduction of D and ^{3}He after the epoch of nucleosynthesis; (iv) the diffuse X-ray and gamma-ray background; (v) the positron production.

6.1. THE CRITICAL DENSITY ρ_c

The most general constraint is imposed by the condition $\rho_X(t_0) + \rho_\nu(t_0) < \rho_c = 1.9 \times 10^{-29}$ g/cm^3. It holds in particular for $X \to 3\nu$ decay. The energy density of neutrinos can be easily found from eq. (36). After simple calculations using eqs. (31), (32) and (36) one finds the following upper limits on E_ν:

$$E_\nu < 3 \times 10^4 (x_f/0.1 r_\nu)^{1/2} N_{200}^{1/4} (\tau_X/t_0)^{1/4} \text{ GeV}, \quad \text{for } t_a \ll \tau_X \ll t_{eq}, \quad (41)$$

$$E_\nu < 9 \times 10^3 (x_f/0.1 r_\nu)^{1/2} N_{200}^{1/4} (\tau_X/t_0)^{1/3} \text{ GeV}, \quad \text{for } t_{eq} \ll \tau_X \ll t_0, \quad (42)$$

$$E_\nu < 8.5 \times 10^3 (0.1 r_\nu/x_f)^{1/2} N_{200}^{1/4} \text{ GeV}, \quad \text{for } \tau_x > t_0, \quad (43)$$

where r_ν is the fraction of X-particle mass converted into energy. Therefore, the neutrino flux (40) can exist only at energies limited by eqs. (41)–(43).

6.2. THE DISTORTION OF THE 2.7 K MICROWAVE RADIATION

The decay of X-particles at the time between $t_{kin} \approx 3 \times 10^5$ s and $t_{dec} \approx 3.6 \times 10_s^{12}$ distorts the 2.7 K microwave radiation. Here t_{kin} is the time when the thermodynamic equilibrium in the Universe is broken, but the kinetic equilibrium

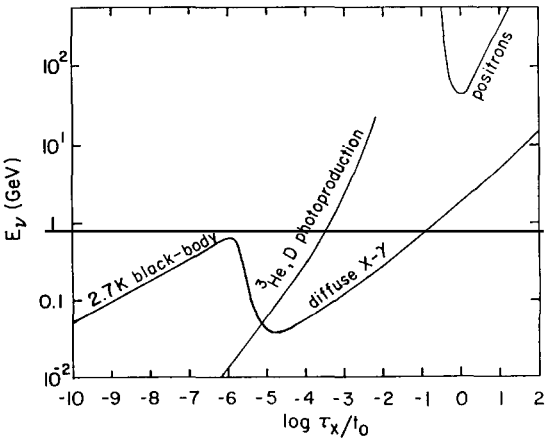

Fig. 1. The upper limits on the neutrino energy E_ν as a function of the X-particle lifetime τ_X. Here $t_0 = 2.1 \times 10^{17}$ s is the age of the universe, and the values x_f, r_{em}, b_ν and N_f are taken as in eqs. (41)–(50). The limit from positron production is given under the assumption of a uniform distribution of X-particles in the universe, with positron branching ratio $b_e = \frac{1}{4}$. The upper limit from diffuse radiation at $\tau_X \gg t_0$ increases as $\tau_X^{1/2}$ until it reaches the value $E_\nu = 8.5 \times 10^3$ GeV imposed by the critical density.

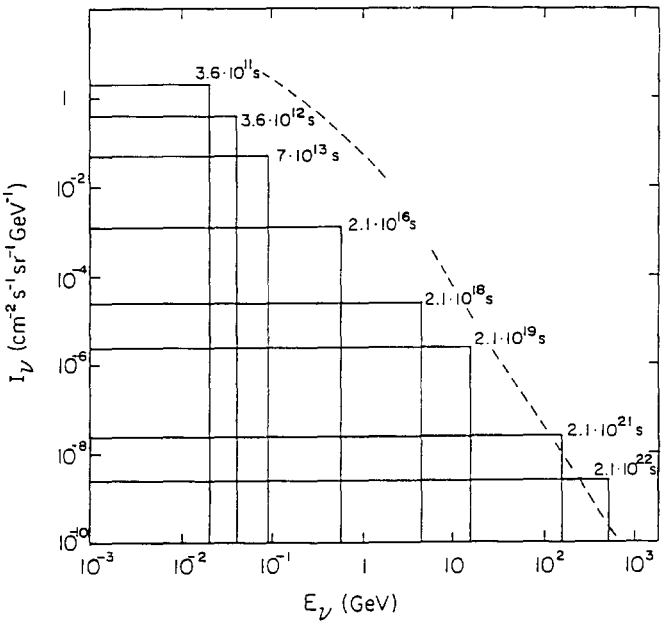

Fig. 2. Differential neutrino fluxes $I_\nu(E)$ for different X-particle lifetimes τ_X (shown at the right corner of each box). The vertical line shows the upper limit of E_ν for a given τ_X. The horizontal line gives the differential neutrino flux according to eq. (40). Note that it is not a spectrum: each point on the horizontal line gives the averaged flux for the mean energy given by eq. (39). The dashed line shows the spectrum of atmospheric neutrinos according to refs. [21,22]. The flux from the decay of X-particles can exceed the atmospheric flux at $E \simeq 0.1$–10 TeV.

is still supported by binary reactions. The energy density deposited to the electron–positron plasma by the decays of X-particles can be calculated as

$$W_{\rm dec} = r_{\rm em}\int_{t_{\rm kin}}^{t_{\rm dec}} \frac{{\rm d}t}{\tau_X} n_X(t) m_X \left(\frac{a(t)}{a(t_{\rm dec})}\right)^4, \tag{44}$$

where $r_{\rm em}$ is fraction of X-particle mass transferred to the electromagnetic component. The weakest bound corresponds to the very general requirement $W_{\rm dec} < (1+z)^4 W_{\rm bb}$ where $W_{\rm bb} \simeq 0.25$ eV/cm^3 is the current ($z = 0$) energy density of the black-body radiation. The corresponding upper limit for E_ν is given in fig. 1 for $r_{\rm em} \simeq 0.5$. Since it makes the neutrino flux unobservable for the range $t_a < \tau_X < t_{\rm dec}$ (see fig. 2), we are not much interested to strengthen this limit further. However, just as a matter of academic concern, we shall give a rough estimate for a reduction factor. Since $z_{\rm kin} \gg z_a$ (see sect. 1), the cascade photons, originated as products of X-decays, do not reach the kinetic equilibrium with the ambient electrons. The black-body spectrum is distorted by the Compton radiation of

electrons and electron–positron pairs from the cascade. The distortion is described by the Compton y-parameter: $\delta W_{bb}/W_{bb} \simeq 10y$, where y is observationally constrained [15] to $y \lesssim 10^{-3}$. Therefore, $\delta W_{bb} \lesssim 10^{-2} W_{bb}$. Taking into account that only part of W_{dec} is transferred to the electrons radiating in the energy interval at interest, one can expect that the curve "2.7 black-body" in fig. 1 can be lowered by one or two orders of magnitude.

6.3. THE PHOTOPRODUCTION OF D AND ^{3}He

Since nucleosynthesis occurs at $t_n \simeq 200$ s ($z_n \simeq 10^8$), much earlier than the epoch of neutrino transparency, it cannot stringently bound the neutrino flux. A much stronger limit is imposed by D- and He-photoproduction [15]. High-energy electrons or photons, produced by X-decays, initiate an electromagnetic cascade. In the low-energy region, where the production of D and ^{3}He occurs, the cascade develops due to e^+e^- production by photons in γp collisions, while electrons radiate photons in inverse-compton scattering on black-body photons. D and ^{3}He are produced by photofission of ^{4}He. This production is effective at $t < t_r \approx 5.4 \times 10^{13}$ s, when the column density of the Universe is greater than x_{rad}.

Instead of a conventional Monte Carlo computation we shall suggest here a simple analytical method to calculate the D and ^{3}He production on ^{4}He. Let us consider the primary electron (the primary photon makes no difference for the calculations given below), produced in $X \to e + \text{all}$ decay. The energy of the electron is $E_0 = f_e m_X$. By scattering off black-body photons it produces the spectrum of the first-generation photons, $N_\gamma^{(1)}(E_\gamma)$. These photons are absorbed in the gas, producing e^+e^- pairs ($\gamma + p \to p + e^+ + e^-$). Then electrons and positrons produce the second-generation photons $N_\gamma^{(2)}(E_\gamma)$ on black-body photons and so on. As shown in appendix B, the spectrum of photons in each generation is approximately given by

$$N_\gamma(E_\gamma, E_0) \simeq 0.1 E_0/E_\gamma^2. \tag{45}$$

Each generation of photons exists for a time τ_a until they are absorbed (due to $\gamma + p \to p + e^+ + e^-$ scattering) in the gas (note that the lifetime of the electrons is much smaller because they scatter on the much more numerous relic photons). The time τ_a is

$$\tau_a = x_{rad}/\rho_g(t)c, \tag{46}$$

where $x_{rad} = 66.6$ g/cm^2 and $\rho_g(t)$ are the radiation length and the density of the gas in the universe, respectively. Interacting with ^{4}He during the time τ_a, each generation of photons produces D and ^{3}He in the reactions $\gamma + {}^4\text{He} \to p + n + D$

and $\gamma + {}^4\mathrm{He} \to {}^3\mathrm{He} + \mathrm{n}$. The number of D nuclei, for example, produced per unit volume and unit time by the ν_g generations of photons is

$$\Delta n_D \simeq 0.1 b_e f_e \nu_g \frac{n_x}{\tau_x} m_x \int \frac{dE}{E^2} \sigma_{ph}(E) n_{He} c \tau_a, \tag{47}$$

where b_e is the branching ratio of electronic decay and $\tau_{ph}(E)$ is the cross section of photofission.

Note that $\Delta n_D / n_{He}$, the number of D nuclei produced by one He nucleus per s, does not depend on time since it is proportional to $n_X \tau_a \propto \rho_X(t)/\rho_g(t)$, where $\rho_X(t) = m_X n_X(t)$ and $\tau_a \simeq 1/\rho_g(t)$. Integrating $\Delta n_D / n_{He}$ over time gives a factor τ_X, because at $t > \tau_X$, $n_X(t)$ exponentially decreases. Therefore, one finally obtains

$$n_D / n_{He} = 0.1 b_e f_e \nu_g (\rho_X / \rho_g) x_{rad} \langle \sigma_{ph}/E \rangle, \tag{48}$$

where

$$\langle \sigma_{ph}/E \rangle = \int_{E_{th}}^{\infty} \frac{dE}{E^2} \sigma_{ph}(E). \tag{49}$$

The picture given above holds until $\rho_g(t) c H^{-1}(t) > x_{rad}$ which implies $\tau_X < 5.4 \times 10^{13}$ s. For larger τ_X the ratio (48) decreases as $\tau_X \ln^{-1} \tau_X$.

For the cross section $\sigma_{ph}(E)$ we used the measurements of refs. [17] (for the production D) and [18] (for the production of ^{3}He). For the value $\langle \sigma/E \rangle$ we obtain 3.3×10^{-3} and 2.2×10^{-2} mb/MeV for D and ^{3}He, respectively. And finally, using the eqs. (31)–(34) and (39) one finds the upper limit for E_ν. In fig. 1 it is plotted against τ_X for the values $\mathrm{D}/{}^4\mathrm{He} < 5 \times 10^{-5}$ and ${}^3\mathrm{He}/{}^4\mathrm{He} < 5 \times 10^{-4}$. For the number of cascade generations we used $\nu_g = 2$ as explained in appendix B.

6.4. THE DIFFUSE X- AND GAMMA-RAYS

As τ_X becomes larger than $t_r \approx 5.4 \times 10^{13}$ s, the most restrictive constraints are imposed by the diffuse X- and γ-rays observed between 1 keV and ~ 100 MeV. For the light X-particles with $m_X < 100$ GeV the background is produced directly through $X \to \gamma +$ all decays or through $X \to e +$ all decays followed by Compton scattering of the electrons off the black-body photons. For $m_X > 100$ GeV the photons and the electrons from X-particle decays initiate electromagnetic cascades. Most of the cascade photons get into the observed energy band. The present-day ($t = t_0$) energy density of electromagnetic radiation produced by X-decays is given by eq. (44) with the upper and lower limits of the integration replaced by t_0 and t_{dec} respectively. This energy density must be less than W_{cas}, constrained by observations of diffuse gamma-radiation (see appendix A and fig.

A.2). Numerically, W_{cas} ranges from 10^{-4} eV/cm^3 for $\tau_X > 1.4 \times 10^{17}$ s down to 2×10^{-6} eV/cm^3 for $\tau_X < 4.2 \times 10^{13}$ s.

The upper limits on neutrino energy due to diffuse X-rays and gamma radiation are plotted in fig. 1. From this figure one observes that for $\tau_X < t_0$ the neutrino energy does not exceed $E_\nu \simeq 1$ GeV. At $\tau_X > t_0$ the upper limit for E_ν increases as $\tau_X^{1/2}$,

$$E_\nu < 1.5\left(\frac{x_f}{0.1}\right)^{1/2}\left(\frac{r_{em}}{0.5}\right)^{-1/2} N_{200}^{5/8}\left(\frac{\tau_X}{t_0}\right)^{1/2} \text{ GeV}, \tag{50}$$

until it reaches the value $E_\nu = 8.5 \times 10^3$ GeV imposed by the critical density (see eq. (43)).

6.5. POSITRONS

If X-particles uniformly fill the universe, they will produce a high-energy positron flux with an equilibrium space density

$$n_e(E) = b_e n_X/(\tau_X b_0 E^2), \tag{51}$$

where b_e is the positron branching ratio and $b_0 E^2$ is the energy loss of the positron per unit time due to inverse-compton scattering off black-body photons ($b_0 = 2.55 \times 10^{-17}$ GeV/s if E is in GeV). Using the observations of the positron flux at $E \sim 1$ GeV we obtained the upper limit for neutrino energy plotted in fig. 1 for $b_e = \frac{1}{4}$. It is considerably less restrictive than the one due to diffuse X-rays and gamma radiation.

As the other extreme case, one can assume that X-particles uniformly fill the galactic halo with the enhanced density $\rho_{halo}/\rho_{inter} \sim 10^4$, as is assumed for dark matter. The flux of positrons increases in this case by a factor $(\rho_{halo}/\rho_{inter})(\tau_{ex}/\tau) \simeq 10^3$, where $\tau_{ex} \simeq 10^8$yr is the characteristic exit time for GeV positrons from halo and $\tau_C \simeq 1/(b_0 E)$ is the inverse-Compton time which determines the lifetime of positrons in extragalactic space. However, even in this case, the X- and γ-ray diffuse limit becomes lower than the positron one at large τ_X, since the latter is proportional to τ_X, while the former is proportional to $\tau_X^{1/2}$.

Antiprotons bind the neutrino energy less severely (the appropriate calculations can be found in ref. [19]).

6.6. NEUTRINO FLUXES AND ENERGIES

Now we can present the neutrino fluxes (40), together with the derived upper limits for the neutrino energies. These fluxes are plotted in fig. 2 for the values of

τ_X attached to each horizontal line. A vertical line shows the upper limit for E_ν calculated for the given values of τ_X. The flux is given by the horizontal line. As m_X varies, it can correspond to any value of energy between E_{max}, given by the vertical line, and $E \ll E_{max}$. Note that the graph gives only the mean flux for the mean neutrino energy. The spectrum must be calculated taking into account the neutrino spectrum from the decay of the X-particle and the distribution of red-shifts at which the decays occur. The flux of atmospheric neutrinos is shown in fig. 2 by the dotted line. The low-energy flux is taken from ref. [20], the high-energy flux from ref. [21], for the vertical direction. Fig. 2 shows the neutrino flux from X-particles can exceed the flux of atmospheric neutrinos at 0.1–10 TeV. The signal from decaying particles reveals itself as a bump in the continuous spectrum of atmospheric neutrinos.

7. The gravitino

7.1. NEUTRINO AND GAMMA-RAY FLUXES

Unless gravitino is the lightest supersymmetric particle (LSP) its lifetime is too short to produce detectable neutrino flux. In the case that the gravitino is the LSP it can decay due to R-parity violation and produce neutrinos. Using eq. (30) for the gravitino space density, we find the neutrino flux at $t = t_0$

$$I_\nu(t_0) = I_0[\exp(-t_a/\tau_G) - \exp(-t_0/\tau_G)], \tag{52}$$

with

$$I_0 = \frac{c}{4\pi} b_\nu n_0 N^{1/4} \frac{t_{eq}^{1/2} t_{dec}^{3/2}}{t_0^2} \frac{T_R}{m_{Pl}} = 3.3 \times 10^8 b_\nu \frac{T_R}{m_{Pl}} \text{cm}^{-2}\ \text{s}^{-1}\ \text{sr}^{-1}, \tag{53}$$

where

$$n_0 = 0.24^2 \left(\frac{45}{16\pi^3}\right)^{5/4} \alpha_s(T_R) N_R^{-1/2} m_{Pl}^{3/2} t_{dec}^{-3/2} = 3.3 \times 10^9\ \text{cm}^{-3}. \tag{54}$$

$\alpha_s(T_R) = 1/24$ and $N_R = 250$ were used for the numerical estimates.

One observes from eq. (53) that the total neutrino flux at $\tau_G \leq t_0$ depends only on the reheating temperature. The upper limits on T_R were derived using the same approach as for the X-particles. These limits are shown in fig. 3. At $\tau_G \gg t_0$ they give

$$\frac{T_R}{m_{Pl}} \frac{m_G}{100\ \text{GeV}} < 1 \times 10^{-15} \frac{0.5}{r_{em}} \frac{\tau_G}{t_0}. \tag{55}$$

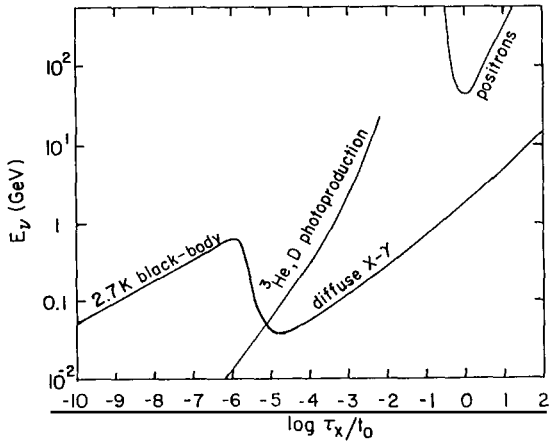

Fig. 3. Upper limits on the reheating temperature T_R as a function of gravitino lifetime τ_G. The limit from positron production is given for $b_e = 0.1$ and for the assumption of a uniform distribution of gravitinos in the universe.

Combining this relation with eqs. (52) and (53) we arrive at

$$I_\nu < 3.5 \times 10^{-7} \frac{0.5}{r_{em}} b_\nu \text{ cm}^{-2} \text{ s}^{-1} \text{ sr}^{-1}. \tag{56}$$

This limit does not depend on τ_G because according to eq. (52), $I_\nu \simeq t_0/\tau_G$, while $T_R \simeq \tau_G/t_0$. If a gravitino with mass $m_G \simeq 100$ GeV decays into two particles as discussed in ref. [9], the flux (56) corresponds to monochromatic neutrinos with energy $E_\nu = \frac{1}{2}m_G \simeq 50$ GeV. The flux of atmospheric neutrinos at this energy is [21] 3.3×10^{-7} cm^{-2} s^{-1} sr^{-1} GeV^{-1} and for a detector with 10% energy resolution, the background for the neutrino line is 1.7×10^{-6} cm^{-2} s^{-1} sr^{-1}, somewhat higher than eq. (56).

The decay gravitino $\rightarrow$ photon + other particle results in the same flux as eq. (56) with b_ν substituted by b_γ. The gamma-ray flux (56) in the form of a gamma-line with $E_\gamma = \frac{1}{2}m_G$ can be detected by a satellite detector such as EGRET. The decay $G \rightarrow \nu + \gamma$, when both particles can be detected, is especially interesting.

The upper limit (56) on neutrino and gamma-ray flux depends on the mechanism of R-parity breaking which provides the ratio b_ν/r_{em} in eq. (56). For example, if R-parity is spontaneously broken and a massless Goldstone boson is produced as a physical particle, Majoron J, (see e.g. the model in ref. [22]), the decay channel $G \rightarrow \nu + J$ can strongly dominate all other decay channels. This case is similar to the decay of a neutralino to a neutrino and Majoron considered in ref.

[23]. It is easy to see that production of other particles occurs as radiative corrections to this process in tree diagrams (e.g. $G \to J + \nu + e^+ + e^-$, $G \to J + \nu + q + \bar{q}$, etc.) and thus they are strongly suppressed ($r_{em} \simeq 10^{-6}$). As a result, the flux in the neutrino line with $E_\nu = \frac{1}{2} m_G$ can be $b_\nu / r_{em} \simeq 10^6$ times higher than the one given by eq. (56).

7.2 GRAVITINO AS THE DARK MATTER

As τ_G / t_0 grows, the upper limit for T_R given by eq. (55) also grows and so does the gravitino space density (19) *. At $T_R / m_{Pl} \simeq 10^{-5}$ it reaches the critical value.

The gravitino as LSP and dark matter particle has a problem, as was already mentioned in ref. [16]. It is connected with the second lightest supersymmetric particle (SLSP). If such a particle is a photino, then it decays to a gravitino and a photon with lifetime $\tau \simeq 10^7$–10^9 s. Our estimates show that the photoproduction of D and ^{3}He on ^{4}He is a factor ~ 10 too high.

There are several ways to ameliorate this difficulty. If the gluino is SLSP, it annihilates stronger and the relic space density of these particles becomes less. However, the most radical possibility is given by a scalar neutrino ($\tilde{\nu}$) as SLSP. In the lowest order, the scalar neutrino decays as $\tilde{\nu} \to G + \nu$, and the D, ^{3}He production is strongly suppressed. This possibility is reversed with respect to the suggestion of ref. [24], where the scalar neutrino is assumed to be LSP and the gravitino SLSP. The relic space density of scalar neutrinos can be readily calculated [5] using the standard technique of ref. [14] and the cross section of $\tilde{\nu} + \tilde{\nu} \to f + \bar{f}$ annihilation. The lifetime of the scalar neutrino,

$$\tau_{\tilde{\nu}} = 4\pi m_{Pl}^2 m_G^{-2} m_{\tilde{\nu}}^{-1} \left(1 - m_G^2 / m_{\tilde{\nu}}^2\right)^{-3}, \tag{57}$$

is of order 10^9–10^{10} s. Therefore, the most restrictive limit on the space density of scalar neutrinos is imposed by the D and ^{3}He production on ^{4}He.

There are two channels for this production. The scalar neutrino can decay radiatively, e.g. $\tilde{\nu} \to G + \nu + e^+ + e^-$, and the products of such a decay, electrons, quarks, etc., initiate an e.m. cascade in which D and ^{3}He are produced. The branching ratio for these decays is too small for the observed abundances of D and ^{3}He.

Another possible channel for cascade's production [25] is connected with neutrino generation in $\tilde{\nu} \to G + \nu$ decay, followed by neutrino absorption by black-body relic neutrinos ($\nu + \bar{\nu}_{bb} \to e^+ + e^-$). It is easy to prove that in our case

* Note that according to eq. (56) the neutrino flux does not change as τ_G (and hence n_G) increases.

this mechanism is even less effective than the one considered above. Indeed, the red-shift of the epoch when transparency for neutrinos with energy $E_\nu = \Delta m \equiv M_{\tilde{\nu}} - m_G$ sets in, according to eq. (12), is equal to $z_a \simeq 3.5 \times 10^7 \ (\Delta m_{100})^{-2/5}$. Therefore, the transparency occurs much earlier than the time of scalar neutrino decay $t \simeq \tau_{\tilde{\nu}}$ and earlier than $t \simeq 7 \times 10^7$, when D and ^{3}He production becomes effective.

The decay of sneutrinos also produces gravitinos. But, as it can be easily shown, their density is considerably less than the critical one.

8. Conclusions

Neutrinos are the deepest probe of the Universe. They allow the search for big-bang relics existing a long time ago. However, the absorption of neutrinos limits the horizon of neutrino detectors to red-shifts $z \simeq 3 \times 10^6$ for 10 MeV neutrinos and $z \simeq 1 \times 10^5$ for 1 TeV neutrinos, while the various upper limits dramatically narrow the range of the properties of the parent particles. Most generally, if $X \to 3\nu$ is not the dominant decay mode, X-particles must be long lived, $\tau_X > t_0$ and have small branching ratios for the decay to positrons and antiprotons.

In our approach we divide the big-bang relics, the neutrino parents, into two groups. The first one is comprised of the particles (which we call X-particles) which were in thermal equilibrium in the early universe. We assume that these particles annihilate by exchange of gauge bosons of $SU(2) \times U(1)$ electroweak group or by exchange of gluons. The second group is comprised of particles for which the thermal equlibrium is not reached. The gravitino, considered in this paper, is an example.

We derived the upper bounds for neutrino energies and neutrino fluxes from X-particle decays. The strongest limits result from the production of isotropic X-ray and gamma-ray radiation (up to $E_\gamma \simeq 100$ MeV). Neutrino energies E_ν are less than ~ 1 GeV for $\tau_X \simeq 3 \times 10^7 t_0$. Detectable neutrino fluxes can exist at 0.1 TeV $< E_\nu <$ 10TeV.

In the case of two-particle decay, $X \to \nu +$ other particle and $X \to \gamma +$ other particle, the detectable neutrino- and gamma-line are produced at $E = \frac{1}{2} m_X$.

The second strongest limit is imposed by the production of positrons and antiprotons, if X-particles are accumulated in the galactic halo. However, this limit is model dependent and at $\tau_X \gg t_0$ it is weak then the one due to the diffuse X- and γ-rays.

The gravitino, if it is LSP, can produce the detectable gamma-ray and (or) neutrino line with energy $E = \frac{1}{2} m_G$. If the R-parity violation is such that all channels of gravitino decay have branching ratios of the same order of magnitude,

effective restrictions can be imposed on the reheating temperature T_R and thus on the gamma-ray and neutrino fluxes. Even in this case, for $m_G \simeq 100$ GeV the intensity of the gamma-ray line at $E_\gamma \simeq 50$ GeV, $I_\gamma \simeq 3 \times 10^{-7}$ cm^{-2} s^{-1} sr^{-1} is a quite prominent feature in the gamma-ray background. The neutrino line at $E_\nu \simeq 50$ GeV can also be marginally detected. However, in some realistic scenarios for R-parity violation (e.g. the model of ref. [22]), the decay mode $G \to J + \nu_L$ (J is the Majoron) strongly dominates over all other channels of the gravitino decay. The neutrino flux in this case can be six orders of magnitude higher [23] and it should be searched for with the help of existing underground detectors such as Kamiokande and IMB.

If gravitinos with $m_G \simeq 100$ GeV are LSP, they can make up the dark matter in the universe. For the realization of this possibility the second lightest supersymmetric particles (SLSP) should be the scalar neutrino. It decays as $\tilde{\nu} \to G + \nu$, thus not overproducing D and ^{3}He, as the photino does if it were SLSP.

Part of this work was done during my visit to the Bonn University. I wish to thank the Humboldt Foundation for the great honour of conferring on me the Humboldt award and my colleagues in Bonn University for warm hospitality. Special thanks are to Prof. G. von Gehlen for many interesting discussions. I am grateful to an anonymous referee for many valuable remarks and for a detailed critical study of the manuscript.

Note added in proof

In this note I would like to compare the approach and the main results of three recent papers on the discussion of high-energy neutrinos from big-bang relics (the other two are the refs. [6,7]).

In ref. [6] very heavy particles, the lightest technicolour baryon and the lightest crypton, are considered. The mass of the former is O(TeV), the mass of the latter can reach O(10^{10} GeV). The authors have obtained the constraints on the relic abundance of these particles using the same phenomena as in the present paper. Since under some assumptions the high energy neutrino observations give the strongest limit, one concludes that the detectable high energy neutrino flux can be produced.

In ref. [7] very heavy particles with masses up to 10^{14} TeV are considered. Their relic abundance at present is taken ad hoc, as in ref. [2], and is constrained by high energy neutrino observations by the Frejus, IMB and Fly's Eye detectors. It implies that the detectable neutrino flux can be produced. As a result, an exclusion plot in space m_X–τ_X/b_ν is obtained, where m_X is a mass of a particle, τ_X is a lifetime and b_ν is a branching ratio for neutrino decay. Implicitly, the authors considered the case $b_\nu = 1$, otherwise a much stronger limit due to diffuse X-ray and gamma radiation is produced.

A natural question can be addressed for both of these works. Since the cross section for annihilation of these very heavy particles is $\langle \sigma v \rangle_{\text{ann}} \sim 1/m_X^2$ and the relic abundances $n_X \sim 1/\langle \sigma v \rangle_{\text{ann}}$, the X-particles must have at present a density higher than the critical one. The solution of this problem, as mentioned in ref. [6], is an entropy production due to the decay of other new particles after decoupling of X-particles. It can result in the dilution of X-particles down to the critical density or below it.

In contrast to the above references, in the present work the following three assumptions are made:

(i) The validity of the standard cosmology (more specifically: all other particles, except the X-particle, are assumed to belong to the content of MSSM),

(ii) The cross section of annihilation $\langle \sigma v \rangle_{\text{ann}} \sim 1/m_X^2$,

(iii) The branching ratios, although they are kept explicitly as b_ν, b_e, b_γ etc., are assumed to be of the same order of magnitude in numerical calculations. As a matter of fact only one assumption is essential: no burst of entropy production occurred after decoupling of X-particles. Surprisingly enough, it results in the conclusion that a detectable neutrino flux can be produced only by long-lived X-particles ($\tau_X \gg t_0$). Due to this assumption the mass of X-particle and the predicted flux are lower than in refs. [6,7].

The neutrino absorption is also considered in ref. [7]. Basically both calculations agree between themselves and with the early results of refs. [4,27].

Appendix A

UPPER LIMITS ON THE ENERGY DENSITY OF THE ELECTROMAGNETIC CASCADE IN THE UNIVERSE

High energy electrons or photons initiate in the intergalactic space an electromagnetic cascade which develops due to pair production $\gamma + \gamma_{bb} \to e^+ + e^-$ and inverse Compton scattering $e + \gamma_{bb} \to e' + \gamma'$ on photons (α_{bb}) of the relic black-body radiation. This phenomenon was first noted in 1969 independently by Hayakawa and Rosenthal. Some of the cascade photons occur in the X-ray and low-energy gamma-ray range and the comparison with observational data allows us to put upper limit on the energy deposition in high-energy photons and electrons. It is connected with the problem considered in this paper: the energy deposition due to the decay of the relic X-particle must not distort the observed isotropic X-ray and gamma-ray ($E_\gamma \simeq 100$ MeV) radiation.

The critical parameter of the cascade is the minimal absorption energy of a photon. The absorption can occur due to $\gamma\gamma$ collisions with optical or black-body radiation (see fig. A.1, taken from ref. [27]). As follows from this figure, if X-particles decay before $t_c \approx 1.4 \times 10^{17}$ s, the daughter photons with energies

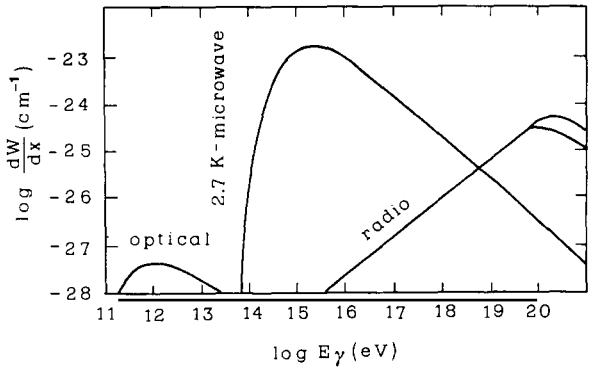

Fig. A.1. Absorption of high-energy photons in the Universe on optical, microwave and radio radiations according to ref. [26]. Here dW/dl is the probability of absorption per unit length. The line $dW/dl = 1 \times 10^{-28}$ cm corresponds to the horizon.

$1 \times 10^{11} < E_\gamma < 6 \times 10^{13}$ eV are absorbed on optical radiation. For the decays at $t > t_c$ the absorption occurs on black-body radiation and the minimum absorption energy is $\epsilon_0 = 7.8 \times 10^{13}$ eV. The spectrum of cascade photons has a cut-off at the energy of absorption.

For the spectrum of cascade photons we shall use the analytical calculations of ref. [26]. There are two characteristic energies in the spectrum: the cut-off energy ϵ_γ and

$$\epsilon_X = \tfrac{1}{3}(\epsilon_\gamma / m_e)^2 \epsilon_{bb}, \tag{A.1}$$

where $\epsilon_{bb} = 6.3 \times 10^{-4}$ eV is the mean energy of black-body photons. At $E < \epsilon_X$ the space density of the cascade photons is

$$n_\gamma(E) = K\epsilon_X^{-1}(E/\epsilon_X)^{-1.5}, \tag{A.2}$$

and at $E > \epsilon_X$

$$n_\gamma(E) = K\epsilon_X^{-1}(E/\epsilon_X)^{-2}, \tag{A.3}$$

where the constant K is related to the energy density of the cascade photons as

$$W_{cas} = K\epsilon_X(2 + \ln \epsilon_\gamma/\epsilon_X). \tag{A.4}$$

To obtain the upper limit on W_{cas} we shall use the upper limit on the isotropic diffuse gamma-ray flux from ref. [27]:

$$I_\gamma^{is}(100 \text{ MeV}) < 1 \times 10^{-7} \text{ cm}^{-2} \text{ s}^{-1} \text{ sr}^{-1} \text{ MeV}^{-1}. \tag{A.5}$$

If the cascade is initiated at $t \sim t_c \approx 1.4 \times 10^{17}$ s (it corresponds in our case to the lifetime of the X-particle $\tau_X > t_c$), we can neglect the absorption on optical radiation. Then we have $\epsilon_\gamma = \epsilon_0 \approx 7.8 \times 10^{13}$ eV and from eqs. (A.1)–(A.5) obtain:

$$W_{cas} < 4 \times 10^{-4} \text{ eV/cm}^3. \tag{A.6}$$

If the cascade is initiated at $t < t_c$, the cut-off is caused by optical radiation ($\epsilon_\gamma \approx 100$ GeV) and eqs. (A.1)–(A.4) result in

$$W_{cas} < 5 \times 10^{-6} \text{ eV/cm}^3. \tag{A.7}$$

Let us now consider the cascade produced at arbitrary red-shift z. Since most probably the galaxy formation occurred at $z < 10$ we can neglect optical radiation at this epoch and consider the cascade development on black-body relic radiation. The spectrum cut-off at the epoch z, $\epsilon_\gamma(z) = \epsilon_0/(1+z)$, is red-shifted to energy

$$\epsilon_\gamma = \epsilon_0/(1+z)^2, \tag{A.8}$$

at $z = 0$. The energy ϵ_X at the epoch z is

$$\epsilon_X(z) = \frac{1}{3}\left(\frac{\epsilon_0}{m_e(1+z)}\right)^2 (1+z)\epsilon_{bb}, \tag{A.9}$$

and at the epoch $z = 0$,

$$\epsilon_X = \epsilon_X(z)/(1+z) = \frac{1}{3}\left(\frac{\epsilon_0}{m_e}\right)^2 \epsilon_{bb}(1+z)^{-2}. \tag{A.10}$$

The density of cascade photons is given by eqs. (A.2)–(A.4). For $z > 2.2 \times 10^2$, $\epsilon_\gamma < 10^9$ eV and $\epsilon_X < 100$ MeV, the spectrum does not suffer the optical cut-off at the latest epochs and from eqs. (A.3)–(A.5) we obtain

$$W_{cas} < \frac{4\pi}{c} I_\gamma(E_\gamma) E_\gamma^2 \left(2 + \ln 3m_e^2/\epsilon_0\epsilon_{bb}\right) = 2.0 \times 10^{-6} \text{ eV/cm}^3. \tag{A.11}$$

For $27 \le z \le 2.2 \times 10^2$, 1.6×10^9 eV $< \epsilon_\gamma < 1 \times 10^{11}$ eV, the optical cut-off is still absent, but one must use eq. (A.2) instead of (A.3). Then we obtain

$$W_{cas} < \frac{4\pi}{c} I_\gamma(E_\gamma) E_\gamma \sqrt{E_\gamma \epsilon_X} \left(2 + \ln 3m_e^2/\epsilon_0\epsilon_{bb}\right) = 4.4 \times 10^{-4}/(1+z) \text{ eV/cm}^3. \tag{A.12}$$

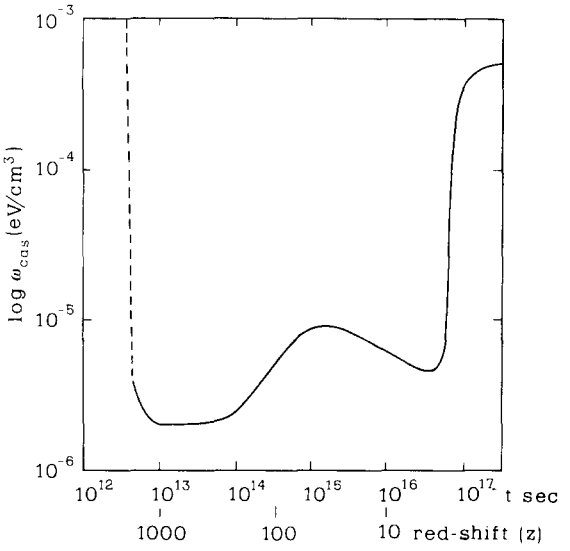

Fig. A.2. Upper limits on the energy density of cascade photons at the present epoch ($z = 0$) for the cascades initiated at the time t (or red-shift z).

The case $(3–5) < z < 27$ needs special consideration. At the time of the cascade development there is probably no optical radiation in the universe. But photons undergo optical absorption at later epochs and the produced electrons reradiate the absorded energy in the slot part of the spectrum. The limit (A.12) then smoothly turns into (A.7).

The derived limits are displayed in fig. A.2; The restrictions due to diffuse X- and gamma-ray background become ineffective for $t < t_{dec} = 3.6 \times 10^{12}\ h^{-1}$ s because the cascade particles are thermalized in this epoch.

As to the problem considered in this paper, W_{cas} ranges from 4×10^{-4} eV/cm^3 for $\tau_X > 1.4 \times 10^{17}$ s to 2×10^{-6} eV/cm^3 for $3.6 \times 10^{12} < \tau_X < 4.2 \times 10^{13}$ s.

Appendix B

THE ELECTROMAGNET CASCADE ON THE BLACK-BODY RADIATION IN THE PRESENCE OF A GAS

In appendix A we considered the electromagnetic cascades which develop due to collisions with black-body photons. At large red-shifts, $z > 300$, the influence of the gas on the cascade development becomes substantial. The number density of black-body photons is, of course, always much larger than the number density of the gas. Therefore, at very high energies when the cascade photons are absorbed

due to $\gamma + \gamma_{bb} \to e^+ + e^-$ collisions, the cascade always develops due the collisions with the black-body photons. However, at small energies the development of a cascade drastically changes due to absorption of photons in the gas.

First we shall list the characteristic values for our problem. The density of gas is $\rho_{gas}(z) = \Omega_B \rho_c/(1+z)^3 = 1.1 \times 10^{-30}(1+z)^{-3}$ g/cm^3, where we assumed for baryonic matter $\Omega_B = 0.1$ and used $H_0 = 75$ (km/s) Mpc. The radiation column density for the gas (77% H and 23% ^{4}He) is $x_{rad} = 66.6$ g/cm^2. The radiation length, $l_{rad} = x_{rad}/\rho_{gas}(z)$, becomes less then the Hubble distance, $cH^{-1}(z)$, at red-shift $z > 3 \times 10^2$. At $E_\gamma < E_c$ the pair production $\gamma + p \to p + e^+ + e^-$ dominates over $\gamma + \gamma_{bb} \to e^+ + e^-$. The critical energy $E_c = 4.7 \times 10^4 (1+z)^{-1}$ GeV is determined by the equality $L_{abs}(E_c) = l_{rad}$ (here L_{abs} is the absorption length due to $\gamma + \gamma_{bb} \to e^+ + e^-$). The characteristic time for Compton energy losses of electrons with Lorentz-factor Γ_e, $\tau_{Comp} = 7.7 \times 10^{19}\, \Gamma e^{-1}(1+z)^{-4}$ s is always considerably less than the time of photon absorption in the gas $\tau_a = 2.1 \times 10^{21}(1+z)^{-3}$ s. Therefore, the electrons radiate their energy away practically instantaneously, while photons of each generation exist in the gas during a time t_a producing the nuclear reactions in the gas. At $E > E_c$ the lifetime of both, photons and electrons, is of order of τ_{Comp} and the time of cascade development is too short for the considerable nuclear production. Now let us proceed with the calculations. Let us begin with the general formula, which will be used in the calculations. If electrons have the spectrum $K_e E_e^{-\gamma_e}$, the photons produced in inverse-Compton scattering have the spectrum

$$N_\gamma(E_\gamma) \propto E_\gamma^{-(\gamma_e/2+1)}. \tag{B.1}$$

Eq. (B.1) follows straightforwardly from the relation between the electron and the Compton-photon energies:

$$E_\gamma = \tfrac{4}{3}(E_e/m_e)^2 \epsilon_{bb}, \tag{B.2}$$

where ϵ_{bb} is the mean energy of the black-body photons. Let us consider an electron with initial energy $E_0 \simeq E_c$ (if $E_0 \gg E_c$, cascade energies degrade down to E_c almost instantaneously). The first-generation photons produced by this electron have the usual inverse Compton spectrum,

$$N_\gamma^{(1)}(E_\gamma) = K_1 E_\gamma^{-3/2}, \tag{B.3}$$

with maximum energy of photons in the spectrum $E_{max}^{(1)} = \xi E_0$, where $\xi \simeq \frac{4}{3} E_c(z)(\epsilon_{bb}(z)/m_e^2) \approx 0.15$. In a time $\tau_a = l_{rad}/c$ these photons produce electrons and positrons, each with energy $E_e \approx \frac{1}{2} E_\gamma$ and thus with the spectral index $\gamma_e = \frac{3}{2}$.

From eq. (B.1) we see that the second-generation photons have the spectrum

$$N_\gamma^{(2)}(E_\gamma) = K_2 E_\gamma^{-7/2}, \tag{B.4}$$

with maximum energy $E_{\max}^{(2)} = 2(\frac{1}{2}\xi)^3 E_0$. The photons of the third generation have spectral index 15/8, the fourth generation photons 31/16 and the nth generation photons have spectrum $K_n E^{-2}$ with maximum energy $E_{\max} = 2(\frac{1}{2}\xi)^k E_0$, where $k = 2^n - 1$. Therefore, we see that the photon spectra of all generations is approximately $N_\gamma(E_\gamma) \approx K E_\gamma^{-2}$. The exceptional case is the first-generation spectrum (eq. (B.3)). However, one should take into account that in reality a cascade in the gas is initiated not by a single electron but by the electrons produced in high energy cascade on black-body photons. These electrons have a spectrum $N_e(E_e) \propto E_e^{-1.5}$ or $N_e(E_e) \propto E_e^{-2}$, which gives according to eq. (B.1) the spectrum of the first-generation photons $N_\gamma(E_\gamma) \propto E_\gamma^{-7/4}$ or $N_\gamma(E_\gamma) \propto E_\gamma^{-2}$, respectively.

Finally, we have to normalize the spectrum. If an electron or a photon produced through X-particle decay has an energy $E_0 > E_c$, the total energy of the cascade particles in each generation is also equal to E_0. Then for the spectrum KE_γ^{-2} we have $E_0 = K \ln E_{\max}/E_{\min}$.

Taking for the logarithm the typical value ~ 10, we obtain the approximate expression for the normalized spectrum of photons in each generation:

$$N_\gamma(E_\gamma) \approx 0.1 E_0 / E_\gamma^2. \tag{B.5}$$

For the production of D and ^{3}He and of ^{4}He, the threshold energy is $E_\gamma \approx 25$ MeV. Then from estimates of the maximum energy in the cascade, given above, one obtains that the number of generations taking part in the D, ^{3}He, production is $\nu_g \simeq 2$–3 depending on E_0 and red-shift z.

Two remarks are in order. The influence of the gas on the development of the cascade is essential only at large red-shifts, $z > 300$ ($t < 5.4 \times 10^{13}$ s), when $l_{\text{rad}} < cH^{-1}(z)$. At $z < 300$ absorption of photons in the gas takes longer than the Hubble time and becomes progressively ineffective as z decreases. The production of D and ^{3}He follows this tendency. Actually I performed more accurate calculations of the spectra, taking into account the contribution of all generations separately as well as the contribution from the cascade on black-body photons. Unfortunately, the analytical expressions are lengthy and have different forms for various red-shifts.

The expression (B.5) provides an accuracy of order of a factor 2 for calculation the ratios D/^{4}He and ^{3}He/^{4}He.

References

[1] V.S. Berezinsky and G.T. Zatsepin, Sov. Phys. Usp. 20 (1977) 361
[2] P.H. Frampton and S.L. Glashow, Phys. Rev. Lett. 44 (1980) 1481

[3] M. Yu. Khlopov and V.M. Chechetkin, preprint, Institute of Applied Mathematics, Moscow (1985)
[4] V.S. Berezinsky, preprint, Bartol Research Institute (Delaware, USA) BA-90-87 (Nov. 1990)
[5] V.S. Berezinsky, Phys. Lett. B261 (1991) 71
[6] J. Ellis et al., preprint CERN-TH-5853/90
[7] P. Gondolo, G. Gelmini and S. Sarkar, preprint UCLA/91/TEP/31
[8] J. Ellis, J.L. Lopez and D.V. Nanopoulos, Phys. Lett. B247 (1990) 257
[9] S. Weinberg, Phys. Rev. Lett. 48 (1982) 1303
[10] J.W.F. Valle, Prog. Part. Nucl. Phys. 26 (1991) 91
[11] J. Ellis et al., Nucl. Phys. B238 (1984) 453
[12] J. Ellis, J.E. Kim and D.V. Napopoulos, Phys. Lett. B145 (1984) 181
[13] V.A. Kuzmin, V.A. Rubakov and M.E. Shaposhnikov, Phys. Lett. B155 (1985) 2822; M.E. Shaposhnikov, Nucl. Phys. B287 (1987) 757
[14] B.W. Lee and S. Weinberg, Phys. Rev. Lett. 39 (1977) 165
[15] H.P. Gush, M. Halpern and E.H. Wishnow, Phys. Rev. Lett. 65 (1990) 537
[16] J. Ellis, D.V. Nanopoulos and S. Sarkar, Nucl. Phys. B259 (1985) 175
[17] A.N. Gorbunov and V.M. Spiridonov, Sov. Phys. JETP 34 (1958) 600
[18] A.N. Gorbunov and V.M. Spiridonov, Sov. Phys. JETP 34 (1958) 596
[19] F.W. Stecker, Nucl. Phys. B252 (1985) 25
[20] G. Barr, T.K. Gaisser and T. Stanev, Phys. Rev. D39 (1989) 3532
[21] K. Mitsui, Y. Minorikawa and H. Komori, Nuovo Cimento C9 (1986) 959
[22] A. Masiero and J.W.F. Valle, Phys. Lett. B251 (1990) 273
[23] V.S. Berezinsky, A. Masiero and J.W.F. Valle, Phys. Lett. B226 (1991) 382
[24] J.A. Frieman and G.F. Giudice, Phys. Lett. B224 (1989) 125
[25] J. Gratsias, R.Y. Scherrer and D.N. Spergel, preprint OSU-TA-9/90
[26] V.S. Berezinsky, S.V. Bulanov, V.A. Dogiel, V.L. Ginzburg and V.S. Ptuskin, Astrophysics of cosmic rays (Elsevier, Amsterdam, 1990)
[27] C.E. Fitchel et al., Ap. J. 222 (1978) 833; D.J. Thompson and C.E. Fitchel, NASA Technical Memorandum 83901 (1982)